

Third-order negative-energy contributions to transition amplitudes in heliumlike ions

I. M. Savukov*

Department of Physics

Princeton University,

Princeton, NJ 08544

L. N. Labzowsky

Department of Physics, St Petersburg State University

Petrodvorets. 198504, St Petersburg, Russia

W. R. Johnson[†]

Department of Physics, 225 Nieuwland Science Hall

University of Notre Dame, Notre Dame, IN 46566

(Dated: March 10, 2005)

Abstract

It is shown that third-order (second-order in the interelectron interaction and first-order in the interaction with the electromagnetic field) contributions to transition amplitudes in heliumlike ions with one negative-energy intermediate state (NES) vanish in QED but not in relativistic many-body perturbation theory (RMBPT). An all-order RMBPT procedure for evaluating transition amplitudes in heliumlike ions that takes this result into account is formulated and used to evaluate $1s2s^3S_1 \rightarrow 1s3s^3S_1$ M1 transitions for heliumlike ions with $Z=2-10$.

PACS numbers: 31.10.+z, 31.30.Jv, 32.70.Cs, 32.80.-t

*Electronic address: isavukov@princeton.edu; URL: <http://www.princeton.edu/~isavukov>

†Electronic address: johnson@nd.edu; URL: <http://www.nd.edu/~johnson>

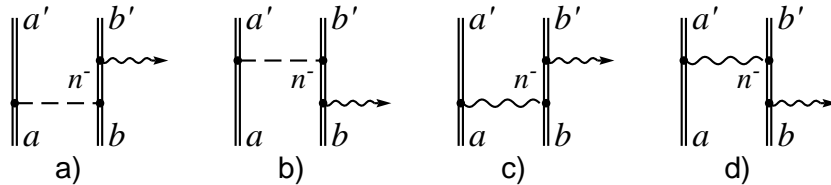


FIG. 1: Feynman graphs for the second-order contribution to the transition probability in a two-electron atom or ion. The double solid lines denote bound electrons. Lower indices a, b denote one-electron initial states while upper indices a', b' denote one-electron final states. Two-electron states ab and $a'b'$ are coupled to give fixed values of angular momentum and parity. The Coulomb gauge is used here; dashed lines denote the Coulomb interaction and wavy lines denote the Breit interaction. The wavy line with an arrow at the end denotes an emitted photon. The index n^- on the internal electron line denotes an intermediate electron state.

I. INTRODUCTION

It has long been known that negative-energy states play an important role in the evaluation of transition probabilities in heliumlike ions [1–6]. Indeed, in a large-scale relativistic configuration-interaction calculation of the intercombination transition in heliumlike carbon by Chen et al. [6], a 50% discrepancy between length and velocity forms was resolved. According to predictions made in [3, 5], the discrepancy vanished after taking into account negative-energy intermediate states. In [1–6], negative energy contributions were included to second order: first order in the interelectron interaction and first order in the interaction with the electromagnetic field. The corresponding Feynman graphs are given in Fig. 1.

In the present paper, we address the same problem in third order (second order in the interelectron interaction and first order in the electromagnetic field). We investigate the problem in both RMBPT and QED. Although NES contributions to transition amplitudes in RMBPT and QED are identical in second-order, they may differ in higher orders. A well-known example, first established in [7], is the sign difference of the second-order energy corrections depicted in Fig. 2. In RMBPT, the contributions from Figs. 2 a) and b) both enter with the same sign, while in QED they have an opposite sign. Moreover, the QED contribution of Fig. 2 c), in contrast to RMBPT, is exactly zero [7]. In higher orders, RMBPT-QED discrepancies become numerous and the only way to correctly account for NES contributions

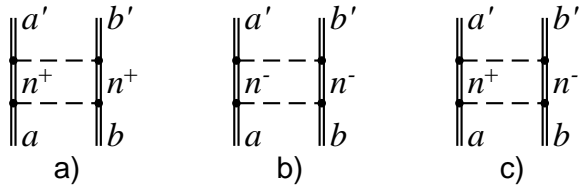


FIG. 2: Feynman graphs for second-order Coulomb energy corrections in He-like ions. The notations are the same as in Fig 1. Positive- and negative-energy contributions are denoted as n^\pm .

is to follow the QED prescription. In this paper, we investigate third-order contributions to transition amplitudes in He-like ions with one negative-energy intermediate state. Although second-order NES contributions to transition probabilities [3, 5, 6] are identical in RMBPT and QED, we show that the net third-order NES contribution from QED vanishes, in sharp contrast to third-order NES contribution from RMBPT.

II. QED DESCRIPTION

We start with a QED description of the third-order contributions to transition probabilities and consider the Coulomb contributions shown in Fig. 3. The contributions from Figs. 3 a) and 3 b) can be reduced to trivial generalizations of contributions Figs. 1 a) and 1 b). Since we consider only one negative state in all of these graphs, the additional Coulomb interactions containing all positive intermediate states will not lead to differences between RMBPT and QED. In principle, one can replace the Coulomb ladder parts of the graphs Figs. 3 a) and 3 b) by a coupled CI wave function as was done in [6]. Less trivial is the situation with the graph Fig. 3 c), and below we will concentrate on an investigation of this graph.

We will be interested in the situation when only one of the internal electron lines contains negative energies. The three corresponding versions of the graph Fig. 3 c) are depicted in Fig. 4. Using the correspondence rules for bound-electron QED (see, e.g. [8]) we can write

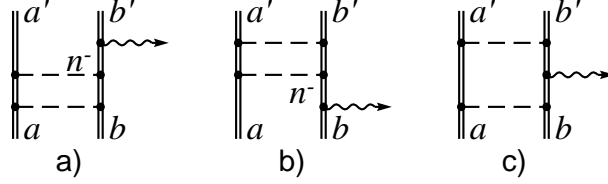


FIG. 3: The third-order Coulomb contributions to the transition probabilities in He-like ions. The notations are the same as in Fig. 1.

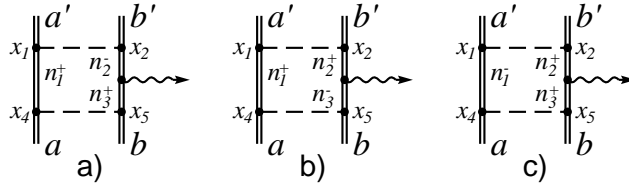


FIG. 4: The versions of the Feynman graph Fig 3 c) with one negative energy intermediate electron state

down an expression for the S-matrix element, corresponding to Fig. 3 c):

$$S_{a'b';ab} = (-i)^5 e^5 \int d^4x_1 \cdots d^4x_5 (\bar{\psi}_{a'}(x_1) \gamma_{\mu_1} S(x_1x_4) \gamma_{\mu_4} \psi_a(x_4)) \times \\ (\bar{\psi}_{b'}(x_2) \gamma_{\mu_2} S(x_2x_3) \gamma_{\mu_3} A_{\mu_3}(x_3) S(x_3x_5) \psi_b(x_5)) D_{\mu_1\mu_2}^c(x_1x_2) D_{\mu_4\mu_5}^c(x_4x_5). \quad (1)$$

In Eq. (1), $\psi_a(x) = \psi_a(\mathbf{r})e^{-iE_a t}$ is the one electron Dirac wave function, E_a is the corresponding eigenvalue, $\bar{\psi}_a$ is the Dirac-conjugated wave function, γ_μ are Dirac matrices. The electron propagator may be written [9]:

$$S(x, x') = \frac{1}{2\pi i} \int d\omega e^{i\omega(t-t')} \sum_n \frac{\psi_n(\mathbf{r})\bar{\psi}_n(\mathbf{r}')}{E_n(1-i0) + \omega}, \quad (2)$$

where the summation is extended over the positive- and negative-energy Dirac spectrum and $i0$ in the denominator defines the usual Feynman contour in the complex ω plane. For the Coulomb photon propagators we employ the expression [8]:

$$D_{\mu_1\mu_2}^c(x, x') = -\frac{i}{|\mathbf{r} - \mathbf{r}'|} \delta(t - t') \delta_{\mu_1 4} \delta_{\mu_2 4}. \quad (3)$$

The photon emission operator A_μ^* (or the photon complex conjugate wave function) is

$$A_\mu^{(\mathbf{k}, \lambda)} = \sqrt{\frac{2\pi}{\omega}} e_\mu^{(\lambda)} e^{i(\mathbf{k}\mathbf{r} - \omega t)}, \quad (4)$$

where \mathbf{k} is the wave vector, $e_\mu^{(\lambda)}$ is the polarization vector, $\lambda = 1, 2$ correspond to transverse polarizations, $\lambda = 3, 4$ correspond to the longitudinal and scalar ones. We use relativistic units $\hbar = c = 1$ and an Euclidean metric in 4-space with an imaginary fourth component: $a_\mu \equiv (\mathbf{a}, ia_4)$. Accordingly, $d^4x \equiv i d\mathbf{r} dt$. The amplitude of the process u_{if} is connected with the S-matrix element by the relation

$$S_{if} = -2\pi i \delta(E_f - E_i) u_{if} \quad (5)$$

where the indices i, f denote the initial and the final states and E_i, E_f are the corresponding total energies of a system. The matrix elements of the amplitude being defined by Eq. (5), the probability of the process is

$$w_{if} = 2\pi \delta(E_f - E_i) |u_{if}|^2 \quad (6)$$

Insertion of the expression for the wave functions and propagators in Eq. (1), integration over the time variables and the use of the formula (5) yields:

$$u_{a'b';ab} = -\frac{ie}{2\pi} \sum_{n_1 n_2 n_3} \int_{-\infty}^{\infty} d\omega' \times \frac{\langle a'b'|V_C|n_1 n_2\rangle \langle n_2|\hat{A}_\omega|n_3\rangle \langle n_1 n_3|V_C|ab\rangle}{(E_{n_1}(1-i0) + \omega') (E_{n_2}(1-i0) - \omega' - E_{a'} - E_{b'}) (E_{n_3}(1-i0) - \omega' - \omega - E_{a'} - E_{b'})}, \quad (7)$$

where V_C is the Coulomb interelectronic interaction $V_C = e^2/|\mathbf{r}_1 - \mathbf{r}_2|$ and \hat{A}_ω is the photon emission operator $\hat{A}_\omega = \sqrt{\frac{2\pi}{\omega}} \mathbf{e} \cdot \boldsymbol{\alpha} e^{i\mathbf{k}\mathbf{r}}$, $\boldsymbol{\alpha}$ is the Dirac matrix and the summation over $n_1 n_2 n_3$ is extended over the complete Dirac spectrum (positive and negative). Consider first the contributions from all positive intermediate electron states. Then in the complex ω' -plane two poles are in the lower half-plane and one pole is in the upper half-plane: $\omega^{(1)} = -E_{n_1} + i0$. Closing the contour of integration in the upper half-plane and using Cauchy's theorem we arrive at the expression

$$u_{a'b';ab}^{(+++)} = e \sum_{n_1^+ n_2^+ n_3^+} \frac{\langle a'b'|V_C|n_1 n_2\rangle \langle n_2|\hat{A}_\omega|n_3\rangle \langle n_1 n_3|V_C|ab\rangle}{(E_{n_1} + E_{n_2} - E_{a'} - E_{b'}) (E_{n_1} + E_{n_3} - E_a - E_b)} \quad (8)$$

In Eq. (8) the singular terms $n_1 n_2 = a'b'$ or $n_1 n_3 = ab$ should be excluded from the summation and treated separately. The investigation of these terms is not our goal in this paper. The contribution $u^{(+++)}$ was included in RMBPT and CI calculations in [3, 5, 6, 10]. It was shown that this contribution, and all higher-order positive-energy contributions, are not

enough to obtain gauge invariance when the operator \widehat{A}_ω is used in the “length” and “velocity” forms. Gauge invariance was restored only when the negative-energy contributions from Fig. 1 were added [5, 6]. Next, we evaluate the contribution of the graph Fig. 4 a). In this case, in the integral over ω' in Eq. (7), two poles are in the upper half-plane and one pole is in the lower half-plane. This latter one is at $\omega'^{(2)} = E_{n_3} - \omega - E_{a'} - E_{b'} - i0$. Closing the contour in the lower half-plane, we obtain

$$u_{a'b';ab}^{(+-+)} = -e \sum_{n_1^+ n_2^- n_3^+} \frac{\langle a'b'|V_C|n_1 n_2\rangle \langle n_2|\widehat{A}_\omega|n_3\rangle \langle n_1 n_3|V_C|ab\rangle}{(E_{n_1} + E_{n_3} - E_a - E_b)(E_{n_2} - E_{n_3} + E_a + E_b - E_{a'} - E_{b'})}. \quad (9)$$

An analogous calculation of the contribution of Fig. 4 b) yields

$$u_{a'b';ab}^{(++-)} = -e \sum_{n_1^+ n_2^+ n_3^-} \frac{\langle a'b'|V_C|n_1 n_2\rangle \langle n_2|\widehat{A}_\omega|n_3\rangle \langle n_1 n_3|V_C|ab\rangle}{(E_{n_1} + E_{n_2} - E_{a'} - E_{b'})(E_{n_3} - E_{n_2} - E_a - E_b + E_{a'} + E_{b'})}. \quad (10)$$

Finally, the contribution of Fig. 4 c) is

$$u_{a'b';ab}^{(-++)} = 0, \quad (11)$$

since in this case all the poles are concentrated in the lower half-plane and the contour can be closed in the upper half-plane.

It should be noted that all Feynman graphs with crossed photons give negligible NES contributions.

III. COMPARISON WITH RMBPT

In RMBPT, the total contribution to the amplitude from the graph Fig. 3 c) for all the positive and negative electron intermediate states is given by Eq. (8) with the summations over $n_1 n_2 n_3$ extended over both positive and negative states. The difference between QED and RMBPT descriptions is evident for $u^{(+-+)}$, $u^{(++-)}$, and $u^{(-++)}$. This difference is highlighted when we replace one of the denominators by $-2m$ and use the completeness of negative energy states in the Pauli approximation. This approximation was used in [5]. Then, employing the closure relation for the nonrelativistic negative states and introducing

the effective emission operator $\widehat{a}_\omega^{C_1}$, we can rewrite Eqs. (9)-(11) in the form

$$u_{\text{QED}}^{(+-+)} = \frac{e}{2m} \sum_{n_1^+ n_3^+} \frac{\langle a'b' | \widehat{a}_\omega^{C_1} | n_1 n_3 \rangle \langle n_1 n_3 | V_C | ab \rangle}{(E_{n_1} + E_{n_3} - E_a - E_b)}, \quad (12)$$

$$u_{\text{QED}}^{(++-)} = \frac{e}{2m} \sum_{n_1^+ n_2^+} \frac{\langle a'b' | V_C | n_1 n_2 \rangle \langle n_1 n_2 | \widehat{a}_\omega^{C_2} | ab \rangle}{(E_{n_1} + E_{n_2} - E_{a'} - E_{b'})}, \quad (13)$$

$$u_{\text{QED}}^{(-++)} = 0, \quad (14)$$

where the effective operators $\widehat{a}_\omega^{C_{1,2}}$ are defined by the relations

$$\sum_{n_2^-} \langle a'b' | V_C | n_1 n_2 \rangle \langle n_2 | \widehat{A}_\omega | n_3 \rangle \equiv \langle a'b' | \widehat{a}_\omega^{C_1} | n_1 n_3 \rangle \quad (15)$$

$$\sum_{n_3^-} \langle n_2 | \widehat{A}_\omega | n_3 \rangle \langle n_1 n_3 | V_C | ab \rangle \equiv \langle n_1 n_2 | \widehat{a}_\omega^{C_2} | ab \rangle. \quad (16)$$

Explicit expressions for $\widehat{a}_\omega^{C_{1,2}}$ are given in [5]. The corresponding RMBPT expressions are found to be

$$u_{\text{RMBPT}}^{(+++)} = -u_{\text{QED}}^{(+-+)} \quad (17)$$

$$u_{\text{RMBPT}}^{(++-)} = -u_{\text{QED}}^{(++-)} \quad (18)$$

$$u_{\text{RMBPT}}^{(-++)} = e \sum_{n_1^- n_2^+ n_3^+} \frac{\langle a'b' | V_C | n_1 n_2 \rangle \langle n_2 | \widehat{A}_\omega | n_3 \rangle \langle n_1 n_3 | V_C | ab \rangle}{(E_{n_1} + E_{n_3} - E_{a'} - E_{b'}) (E_{n_1} + E_{n_2} - E_a - E_b)}. \quad (19)$$

Going over to the Pauli approximation for the summation over n_1^-, n_2^+, n_3^+ and using the closure relation again, we obtain

$$u_{\text{RMBPT}}^{(-++)} = \frac{e}{4m^2} \langle a'b' | \widehat{a}_\omega^{CC} | ab \rangle \quad (20)$$

where the effective emission operator \widehat{a}_ω^{CC} is the sum in Eq. (19) with the denominator replaced by $4m^2$. Returning now to the contributions Figs. 3 a) and b), we find that in the QED approach they exactly cancel the contributions from Fig. 3 c) given in Eqs. (12) and (13). Therefore, the total third-order NES contribution is zero within the QED approach. In the RMBPT approach, on the other hand, the contributions from Figs. 3 a), 3 b), and 3 c) add coherently.

Below, we will combine our QED results with an all order (in the interelectron interaction) calculation. Symbolically, the second-order NES correction can be written as

$$u_{\text{NES1}}^{(2)} = \langle \Psi_0^F | \widehat{a}_\omega^{C_1} + \widehat{a}_\omega^{C_2} | \Psi_0^I \rangle \quad (21)$$

where Ψ_0^F, Ψ_0^I are coupled wave functions for the final (F) and initial (I) states in the one electron approximation. Apparently, we can add an infinite number of Coulomb lines to the graph of Fig. 1 a) from below and to the graph Fig. 1 b) from above, without making any difference between QED and RMBPT:

$$u_{\text{NES1}}^{(\text{all})} = \langle \Psi_\infty^F | \hat{a}_\omega^{C1} | \Psi_0^I \rangle + \langle \Psi_0^F | \hat{a}_\omega^{C2} | \Psi_\infty^I \rangle. \quad (22)$$

where $\Psi_\infty^F, \Psi_\infty^I$ are exact (e.g. CI) wave functions.

The contributions of the Feynman graphs Figs. 3 a) and b) are included in Eq. (22). The NES contribution that arises from addition of the Coulomb ladder to the graph Fig. 3 c) from below and from above may be written

$$u_{\text{NES2}}^{(\text{all})} = [\langle \Psi_0^F | \hat{a}_\omega^{C1} | \Psi_\infty^I \rangle - \langle \Psi_\infty^F | \hat{a}_\omega^{C1} | \Psi_0^I \rangle] + [\langle \Psi_\infty^F | \hat{a}_\omega^{C2} | \Psi_0^I \rangle - \langle \Psi_0^F | \hat{a}_\omega^{C2} | \Psi_\infty^I \rangle]. \quad (23)$$

Here, we took into account the correct sign following from the QED derivation. Combination of both contributions for NES1 and NES2 yields

$$u_{\text{NES}}^{(\text{all})} = u_{\text{NES1}}^{(\text{all})} + u_{\text{NES2}}^{(\text{all})} \quad (24)$$

$$= \langle \Psi_\infty^F | \hat{a}_\omega^C | \Psi_0^I \rangle + \langle \Psi_0^F | \hat{a}_\omega^C | \Psi_\infty^I \rangle - \langle \Psi_\infty^F | \hat{a}_\omega^C | \Psi_\infty^I \rangle, \quad (25)$$

where

$$\hat{a}_\omega^C = \hat{a}_\omega^{C1} + \hat{a}_\omega^{C2}. \quad (26)$$

Expression (25) is convenient for practical calculations since an explicit expression for \hat{a}_ω^C , including angular reduction, was already obtained in [5].

We can check the expression (25) in case when the perturbation theory works well (high Z). Neglecting terms of higher order, we have approximately

$$\begin{aligned} \langle \Psi_\infty^F | \hat{a}_\omega^C | \Psi_0^I \rangle &= \langle \Psi_0^F | \hat{a}_\omega^C | \Psi_0^I \rangle \\ \langle \Psi_0^F | \hat{a}_\omega^C | \Psi_\infty^I \rangle &= \langle \Psi_0^F | \hat{a}_\omega^C | \Psi_0^I \rangle \\ \langle \Psi_\infty^F | \hat{a}_\omega^C | \Psi_\infty^I \rangle &= \langle \Psi_0^F | \hat{a}_\omega^C | \Psi_0^I \rangle. \end{aligned}$$

From this, we obtain

$$u_{\text{NES}}^{(2)} = \langle \Psi_0^F | \hat{a}_\omega^C | \Psi_0^I \rangle \quad (27)$$

in agreement with Eq. 21. In the next order,

$$\begin{aligned}\langle \Psi_\infty^F | \widehat{a}_\omega^C | \Psi_0^I \rangle &= \langle \Psi_0^F | \widehat{a}_\omega^C | \Psi_0^I \rangle + \langle \Psi_1^F | \widehat{a}_\omega^C | \Psi_0^I \rangle \\ \langle \Psi_0^F | \widehat{a}_\omega^C | \Psi_\infty^I \rangle &= \langle \Psi_0^F | \widehat{a}_\omega^C | \Psi_0^I \rangle + \langle \Psi_0^F | \widehat{a}_\omega^C | \Psi_1^I \rangle \\ \langle \Psi_\infty^F | \widehat{a}_\omega^C | \Psi_\infty^I \rangle &= \langle \Psi_0^F | \widehat{a}_\omega^C | \Psi_0^I \rangle + \langle \Psi_1^F | \widehat{a}_\omega^C | \Psi_0^I \rangle + \langle \Psi_0^F | \widehat{a}_\omega^C | \Psi_1^I \rangle,\end{aligned}$$

where Ψ_1^I and Ψ_1^F are the first order in the interelectronic interaction wave functions. Insertion of all these expressions into Eq. (25) yields:

$$u_{\text{NES}}^{(2)} + u_{\text{NES}}^{(3)} = \langle \Psi_0^F | \widehat{a}_\omega^C | \Psi_0^I \rangle \quad (28)$$

i.e.

$$u_{\text{NES}}^{(3)} = 0, \quad (29)$$

in agreement with QED prediction. The all-order NES correction can be obtained from the accurate CI wave functions, which usually are expanded using coupled configuration state functions Φ_K ,

$$\begin{aligned}\Psi_I^{CI} &= \sum_K C_{IK} \Phi_K \\ \Psi_F^{CI} &= \sum_L C_{FL} \Phi_L\end{aligned}$$

Denoting $(\widehat{a}_\omega)_{IJ}$ the matrix elements of the effective operator \widehat{a}_ω between the state functions Φ_I and Φ_J , for which angular reduction is performed, we have:

$$u_{\text{NES}}^{(\text{all})} = C_{II} C_{FF} (\widehat{a}_\omega)_{FI} - \sum_{K \neq I, L \neq F} C_{IK} C_{LF} (\widehat{a}_\omega)_{LK} \quad (30)$$

The principal configuration contribution, the first term that corresponds to second-order correction, comes with an opposite sign compared to the remaining contribution corresponding to third- and higher-order corrections.

IV. BREIT INTERACTION

Consider now the third-order Coulomb-Breit contributions to the transition probabilities in heliumlike ions. We are interested only in the graphs of the type Fig. 3 c). There are two of these graphs which are depicted in Fig. 5. Our formulation will refer to the graph

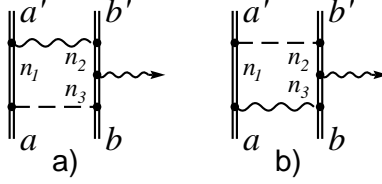


FIG. 5: The third-order Coulomb-Breit contributions to transition probabilities. The notations are the same as in Fig. 1

Fig. 5 a). The derivations for the contribution of the graph Fig. 5 b) are quite similar. The S-matrix element corresponding to the graph Fig. 5 a) differs from Eq. (1) only by changing the first of the Coulomb propagators $D_{\mu_1\mu_2}^c(x_1x_2)$ to a transverse photon propagator:

$$D_{\mu_1\mu_2}^t(x_1x_2) = \int e^{i\omega'(t_1-t_2)} \left\{ \frac{\delta_{\mu_1\mu_2}}{r_{12}} e^{i|\omega'|r_{12}} - \nabla_{1\mu_1} \nabla_{2\mu_2} \frac{1}{r_{12}} \frac{e^{i|\omega'|r_{12}} - 1}{\omega'^2} \right\} (1 - \delta_{\mu_1 4}) (1 - \delta_{\mu_2 4}). \quad (31)$$

Neglecting retardation, i.e. using the operator $V_B(0)$ instead of retarded $V_B(E)$,

$$V_B(E) = \frac{\alpha_1\alpha_2}{r_{12}} e^{i|E|r_{12}} - (\nabla_1 \nabla_2) \frac{1}{r_{12}} \frac{e^{i|E|r_{12}} - 1}{E^2}, \quad (32)$$

and introducing the associated effective emission operator [5],

$$\sum_{n_2^-} \langle a'b' | V_B(0) | n_1 n_2 \rangle \langle n_2 | \hat{A}_\omega | n_3 \rangle \equiv \langle a'b' | \hat{a}_\omega^{B1} | n_1 n_3 \rangle \quad (33)$$

We write down the contribution of Fig. 5 a) in a form similar to Eq. (12):

$$u_{a'b';ab}^{(+-+)} = \frac{e}{2m} \sum_{n_1^+ n_3^+} \frac{\langle a'b' | \hat{a}_\omega^{B1} | n_1 n_3 \rangle \langle n_1 n_3 | V_C | ab \rangle}{(E_{n_1} + E_{n_3} - E_a - E_b)} \quad (34)$$

In static Breit approximation ($V_B(0)$) all of the formulas Eqs. (12)-(16) immediately follow with the replacement of the effective operators $\hat{a}_\omega^{C1,2}$ by the operators $\hat{a}_\omega^{B1,2}$. The formula (19) now becomes

$$u_{\text{RMBPT}}^{(-++)} = \frac{e}{4m^2} \langle a'b' | \hat{a}_\omega^{BC} | ab \rangle, \quad (35)$$

where the operator \hat{a}_ω^{CB} is defined by

$$\langle a'b' | \hat{a}_\omega^{BC} | ab \rangle = \sum_{n_1^- n_2^+ n_3^+} \langle a'b' | V_B(0) | n_1 n_2 \rangle \langle n_2 | \hat{A}_\omega | n_3 \rangle \langle n_1 n_3 | V_C | ab \rangle.$$

We neglect the contribution of the Feynman graphs of the type Fig. 5 with the two Breit interactions which is evidently $(\alpha Z)^2$ times smaller than the contribution with one Breit interaction.

V. NUMERICAL RESULTS

In this section we apply the procedure developed above to $1s2s^3S_1 \rightarrow 1s3s^3S_1$ M1 transitions in low- Z heliumlike ions which are particularly sensitive to NES corrections. The calculations are performed in a Coulomb B-spline basis set. No-pair (positive energy states only) matrix elements are calculated accurately using the relativistic configuration-interaction method. We found that the M1 no-pair results were sensitive to the cavity size and the number of basis functions included in CI. By varying the cavity and the number of basis functions, we found that the optimal parameters are: the cavity size is $50/(Z-1)$ a.u., $n_{\max}=30$, $l_{\max}=2$, which resulted in about 5000 relativistic configurations. The static Breit interaction was included in the CI calculation, and fully retarded M1 matrix elements were used. Expansion coefficients obtained in the no-pair CI calculation were used in the evaluation of NES contributions according to Eq. (30). Since the angular reduction was performed only for states of s -symmetry, we only include the NES contributions from these states, which have dominant weighting coefficients. Results of our numerical calculations are presented in Table I. We found significant disagreement with previous model potential calculations [5] in the case of neutral helium; however, the present results approach rapidly the model potential values as Z increases, unlike the case when only second-order NES corrections are included. We also find that our new helium value based on the current theory agrees better with calculations by Łach and Pachucki [11] ($A = 6.484 \times 10^{-9} \text{ s}^{-1}$) based on Breit-Pauli expansion method and accurate non-relativistic wave functions than did our previous model potential value $A = 1.17 \times 10^{-8} \text{ s}^{-1}$, although some discrepancy still exists, which is not surprising for such a highly non-relativistically forbidden transition. It is interesting to note that naive RMBPT all-order NES contribution 4.793×10^{-6} , defined as $\langle \Psi_{\infty}^F | \widehat{a}_{\omega}^{C1} | \Psi_{\infty}^I \rangle$, is almost twice as large as the correct QED value. As far as spin-changing transitions to the ground state are concerned, as we have shown previously, the Coulomb and Breit NES contributions cancel accurately in second order. Our generalization to infinite order, Eq. (30) would give a very small contribution because the effective operator with the selection rule for total spin vanishes. In other words, although Coulomb and Breit contributions separately will be relatively large and will differ depending on whether second-order or infinite-order theory is employed, the sum will be very small in either case.

TABLE I: Results of calculations for the $1s2s^3S_1 \rightarrow 1s3s^3S_1$ M1 transitions. Notations: Z is the nuclear charge of the heliumlike atom or ion; ω_{np} denotes no-pair relativistic CI transition energy in a.u.; third, forth, and fifth columns contain respectively no-pair CI, NES, and total M1 matrix elements in a.u.; A is the transition rate in s^{-1} ; brackets denote powers of ten

Z	ω_{np}	no-pair	NES	Total	A
2	0.106540	5.896[-6]	2.374[-6]	8.270[-6]	7.86[-9]
3	0.358693	2.547[-5]	6.881[-6]	3.235[-5]	4.59[-6]
4	0.750388	5.767[-5]	1.108[-5]	6.875[-5]	1.90[-4]
5	1.281346	1.025[-4]	1.500[-5]	1.175[-4]	2.76[-3]
6	1.951602	1.598[-4]	1.877[-5]	1.786[-4]	2.25[-2]
7	2.761287	2.297[-4]	2.244[-5]	2.522[-4]	1.27[-1]
8	3.710581	3.123[-4]	2.605[-5]	3.383[-4]	5.56[-1]
9	4.799704	4.074[-4]	2.961[-5]	4.370[-4]	2.01[0]
10	6.028920	5.151[-4]	3.315[-5]	5.483[-4]	6.26[0]

VI. CONCLUSIONS

In this paper, we have considered NES contributions beyond second order using the QED formalism. We discovered that the third-order NES correction is identically zero in the Coulomb basis. Because correlations are very large for low- Z heliumlike ions, especially in the Coulomb basis, we also obtained an expression for all-order NES contributions. We calculated M1 transition rates for low- Z $1s2s^3S_1 \rightarrow 1s3s^3S_1$ transitions and compared them with previous results. All-order NES corrections differ significantly from second-order NES corrections, especially in neutral helium.

Acknowledgments

The work of W. R. J. and I. S. was supported in part by National Science Foundation Grant No. PHY-01-39928. L. L. is grateful to the Notre Dame University for the hospitality

during his stay in 2002.

- [1] G. Feinberg and J. Sucher, Phys. Rev. Lett. **26**, 681 (1971).
- [2] E. Lindroth and S. Salomonson, Phys. Rev. A **41**, 4659 (1990).
- [3] W. R. Johnson, D. R. Plante, and J. Sapirstein, Adv. At. Mol. Opt. Phys. **35**, 255 (1995).
- [4] P. Indelicato, Phys. Rev. Lett. **77**, 3323 (1996).
- [5] A. Derevianko, I. M. Savukov, W. Johnson, and D. Plante, Phys. Rev. A **58**, 4453 (1998).
- [6] M. H. Chen, K. T. Cheng, and W. Johnson, Phys. Rev. A **64**, 042507 (2001).
- [7] L. N. Labzovskii, Sov. Phys. JETP **32**, 94 (1971).
- [8] L. Labzovsky, G. Klimchitskaya, and Y. Dmitriev, *Relativistic Effects in the Spectra of the Atomic Systems* (IOP, Bristol and Philadelphia, 1993).
- [9] A. Akhiezer and V. Berestetskii, *Quantum Electrodynamics* (Interscience, New York, 1965).
- [10] P. Jönsson and C. Froese-Fischer, Phys. Rev. A **57**, 4967 (1998).
- [11] G. Lach and K. Pachucki, Phys. Rev. A **64**, 042510 (2001).